International Journal of Thermophysics, Vol. 21, No. 1, 2000

An Improvement on the Prediction of Optical Constants and Radiative Properties by Introducing an Expression for the Damping Frequency in Drude Model

J. Chen[1,2] and X.-S. Ge[1]

Received April 21, 1999

A method for predicting the optical constants and the radiative properties of metals and heat mirror films, by introducing an expression for the damping frequency in the Drude model, is described. The directional emissivity of aluminum predicted by this method agrees well with the classical experimental values given by Schmidt and Eckert. The prediction of the normal emissivity of indium–tin–oxide (ITO) heat mirror films is in agreement with our measured results. The directional emissivity of copper predicted using this method is reported. The calculated result of the spectrum normal emissivity of copper at 4 μm and 20°C is also given, which supports the measured result. The values for the directional emissivity of aluminum calculated by using various methods based on the Hagen–Rubens relation are reported, and the values do not agree with the experimental results.

KEY WORDS: aluminum; copper; damping frequency; Drude model; optical properties; radiative properties.

1. INTRODUCTION

The thermal radiative properties of optically smooth surfaces and films can be predicted, if their optical constants, refractive index n, and extinction coefficient k are known. The optical constants can be determined by relations based on the dispersion theory that establishes the connection among n, k, and the electrical properties of a material.

[1] Department of Thermal Science and Energy Engineering, University of Science and Technology of China, Hefei 230026, People's Republic of China.
[2] To whom correspondence should be addressed.

0195-928X/00/0100-0269$18.00/0 © 2000 Plenum Publishing Corporation

It is known that, for good conductors in the infrared region, Hagen and Rubens verified on the basis of their experimental study of the reflection of polished metals that n and k are sufficiently high, and moreover, they are closer and closer to each other with an increase in wavelength λ, and the relation $n \approx k$ exists. Thus, from the Drude model together with the Fresnel equations, a simplified formula can be derived to predict the reflectivity in the infrared at normal direction, ρ_λ, as [1–3]

$$\rho_\lambda = 1 - 0.365\sqrt{\frac{1}{\sigma\lambda_0}} \tag{1}$$

where σ is the electrical conductivity and λ_0 is the wavelength in vacuum.

The above-mentioned formula is usually called the Hagen–Rubens equation and was generally introduced to estimate the normal reflectance for metals [4, 5] and for heavily doped oxide semiconducting heat mirror films [6, 7]. However, the use of this relation to predict the normal reflectance of these materials can result in serious error, because the assumption of $n \approx k$ is not entirely satisfied. Additionally, because of the difficulty associated with measurement of the directional emissivity, few experimental data are presented in books on thermal radiation heat transfer [4, 5, 8].

This paper reports a method in which an expression for the damping frequency γ_0 is introduced into the Drude model for predicting the directional emissivity of some materials [9]. We call it the D-R method. Calculated values for aluminum and single layer ITO heat mirror obtained using the D-R method agree well with the experimental values given by Schmidt and Eckert and our experimental data, respectively. It is shown that the results calculated with the Hagen–Rubens relation exhibit an evident departure from the experimental values. The total normal emissivity and the spectrum normal emissivity of copper at 4 μm and 20°C are also given, and they support the experimental results obtained by Eckert and the results reported in Ref. 5, respectively.

2. EMISSIVITY AND RELATIONS BETWEEN THE OPTICAL CONSTANTS AND THE DIELECTRIC FUNCTION

2.1. Relations Between the Emissivity and the Optical Constants

An electromagnetic wave that travels through air (whose refractive index $n \approx 1$) and hits the surface of metal (whose complex refraction index $N = n - ik$) can be resolved into two components of polarization, the perpendicular and the parallel polarized components. The ratios of the complex amplitudes of the reflected electric vectors to the complex amplitudes of the incident electric vectors can be expressed by [10]

$$\mathbf{r}_{s\lambda}(\theta) = -\frac{\sin(\theta - \beta)}{\sin(\theta + \beta)} \tag{2}$$

$$\mathbf{r}_{p\lambda}(\theta) = -\frac{\mathrm{tg}(\theta - \beta)}{\mathrm{tg}(\theta + \beta)} \tag{3}$$

where the subscripts s and p denote the perpendicular and parallel components, respectively. β is the angle of refraction within the metal and can be determined by Snell's law expressed as

$$\sin\beta = \frac{\sin\theta}{N} = \frac{\sin\theta}{n - ik} \tag{4}$$

Substituting Eq. (4) into Eqs. (2) and (3), the reflectivities for the perpendicular and the parallel-polarized components are then obtained as

$$R_{s\lambda}(\theta) = |\mathbf{r}_{s\lambda}|^2 = \frac{(n\cos\beta - \cos\theta)^2 + (k\cos\beta)^2}{(n\cos\beta + \cos\theta)^2 + (k\cos\beta)^2} \tag{5}$$

$$R_{p\lambda}(\theta) = |\mathbf{r}_{p\lambda}|^2 = \frac{(n\cos\theta - \cos\beta)^2 + (k\cos\theta)^2}{(n\cos\theta + \cos\beta)^2 + (k\cos\theta)^2} \tag{6}$$

Equation (4) can be expressed as $\cos\beta = qe^{i\delta}$, where

$$q = \sqrt{\left[1 - \frac{n^2 - k^2}{(n^2 + k^2)^2}\sin^2\theta\right]^2 + \left[\frac{2nk\sin^2\theta}{(n^2 + k^2)^2}\right]^2} \tag{7}$$

$$\delta = 0.5\arctan\frac{2nk\sin^2\theta/(n^2 + k^2)^2}{1 - [(n^2 - k^2)\sin^2\theta/(n^2 + k^2)]} \tag{8}$$

For metals in the region of long wavelength thermal radiation, the following relations are valid:

$$(n^2 + k)^2 \gg 2nk \tag{9}$$

$$(n^2 + k)^2 \gg |(n^2 - k^2)\sin^2\theta| \tag{10}$$

Thus, from Eqs. (7) and (8), we know that $q \to 1$ and $\delta \to 0$ in this region, that is, $\cos \beta \to 1$, and then, Eqs. (5) and (6) can be simplified, respectively, to

$$R_{s\lambda}(\theta) = |\mathbf{r}_{s\lambda}|^2 = \frac{(n - \cos \theta)^2 + k^2}{(n + \cos \theta)^2 + k^2} \tag{11}$$

$$R_{p\lambda}(\theta) = |\mathbf{r}_{p\lambda}|^2 = \frac{(n \cos \theta - 1)^2 + (k \cos \theta)^2}{(n \cos \theta + 1)^2 + (k \cos \theta)^2} \tag{12}$$

For the unpolarized incident radiation, the reflectivity R_λ can be determined by $R_\lambda = 0.5(R_{p\lambda} + R_{s\lambda})$. Hence, according to Kirchhoff's law, the monochromatic emissivity, $\epsilon_\lambda(\theta)$, can be written as

$$\epsilon_\lambda(\theta) = 1 - R_\lambda(\theta) = 1 - 0.5(R_{p\lambda} + R_{s\lambda}) \tag{13}$$

2.2. Relations Between the Dielectric Function and the Optical Constants

The relations between the frequency-dependent complex dielectric function, $\varepsilon^*(\omega) = \varepsilon_1(\omega) + i\varepsilon_2(\omega)$, and the complex refractive index are

$$n^2 - k^2 = \varepsilon_1(\omega) \tag{14}$$

$$2nk = \varepsilon_2(\omega) \tag{15}$$

where ω is the angular frequency, and $\varepsilon_1(\omega)$ and $\varepsilon_2(\omega)$ are the real and imaginary parts of the complex dielectric function, respectively.

Considering that the relations $n \ll k$ and $\varepsilon_1(\omega) < 0$ are valid for metals in the long wavelength thermal radiative region ($\hbar\omega < 0.39$ eV), the refractive index, n, and extinction coefficient, k, can be related to the real and imaginary parts of the complex dielectric function through Eqs. (14) and (15), respectively, as

$$n = \sqrt{\frac{1}{2}\varepsilon_1(\omega)\left[1 - \sqrt{\left(1 + \frac{\varepsilon_2^2(\omega)}{\varepsilon_1^2(\omega)}\right)}\right]} \tag{16}$$

$$k = \sqrt{-\frac{1}{2}\varepsilon_1(\omega)\left[1 + \sqrt{\left(1 + \frac{\varepsilon_2^2(\omega)}{\varepsilon_1^2(\omega)}\right)}\right]} \tag{17}$$

If the real and imaginary parts of the complex dielectric function are known, the optical constants n and k can be determined by Eqs. (16) and (17). The spectral directional emissivity $\epsilon_\lambda(\theta)$ can be obtained based on

Eqs. (11)–(13), and then, the total directional emissivity can, finally, be predicted by

$$\epsilon(\theta) = \frac{\int_0^\infty \epsilon_\lambda(\theta)\, I_{b\lambda} d\lambda}{\int_0^\infty I_{b\lambda} d\lambda} \tag{18}$$

where $I_{b\lambda}$ is the radiation intensity of a black body.

3. THE COMPLEX DIELECTRIC FUNCTION

3.1. The Complex Dielectric Function of Metals

The frequency-dependent complex dielectric function of metals $\varepsilon^*(\omega)$ consists of the intraband excitations due to the free electron-like behavior and the interband excitations associated with bound-electron effects. They thereby can be expressed as follows [11, 12]:

$$\varepsilon^*(\omega) = \varepsilon_1(\omega) + i\varepsilon_2(\omega) = 1 + \chi^f(\omega) + \chi^b(\mathrm{w}) \tag{19}$$

where $\chi^f(\omega)$ is the susceptibility of the free electron and $\chi^b(\omega)$ is the susceptibility of the bound electron. With the help of the Drude model, $\chi^f(\omega)$ can be written in the form

$$\chi^f(\omega) = -\frac{\omega_N^2}{\omega(\omega + i\gamma)} = -\frac{\omega_N^2}{\omega^2 + \gamma^2} + i\frac{\omega_N^2}{\omega}\frac{\gamma}{\omega^2 + \gamma^2} \tag{20}$$

where γ is the damping frequency and $\omega_N^2 = e^2 n_e/\varepsilon_0 m_e$, e is the charge of an electron, n_e is the free electron concentration, ε_0 is the dielectric constant in vacuum, and m_e is the effective mass of electrons. $\chi^b(\omega)$ was well described in the random phase approximate theory and can be expressed as [11, 13]

$$\chi^b(\omega) = \chi_1^b(\omega) + i\chi_2^b(\omega) \tag{21}$$

where $\chi_1^b(\omega)$ and $\chi_2^b(\omega)$ are the real and imaginary parts of $\chi^b(\omega)$. By using Eqs. (20) and (21), the complex dielectric function will be

$$\varepsilon^* = 1 - \left[\frac{\omega_N^2}{\omega^2 + \gamma^2} - \chi_1^b(\omega)\right] + i\left[\frac{\omega_N^2}{\omega}\frac{\gamma}{\omega^2 + \gamma^2} + \chi_2^b(\omega)\right] \tag{22}$$

In the high-frequency region ($\hbar\omega > 4$ eV), $\chi_1^b(\omega)$ tends to be equal to a constant and $\chi_2^b(\omega)$ vanishes [11, 12]. Then Eq. (22) reduces to

$$\varepsilon^* = 1 - \frac{\omega_N^2}{\omega^2 + \gamma^2} + \chi_1^b(\omega) + i\frac{\omega_N^2}{\omega}\frac{\gamma}{\omega^2 + \gamma^2} \tag{23}$$

In the case for $\omega \to \infty$, Eq. (23) becomes

$$\varepsilon^*(\infty) = 1 + \chi_1^{\mathrm{b}}(\omega) = \varepsilon_\infty \tag{24}$$

where ε_∞ is the high frequency dielectric constant. Substituting Eq. (24) into Eq. (23), we have

$$\varepsilon^* = \varepsilon_\infty - \frac{\omega_{\mathrm{N}}^2}{\omega^2 + \gamma^2} + i\,\frac{\omega_{\mathrm{N}}^2}{\omega}\,\frac{\gamma}{\omega^2 + \gamma^2} \tag{25}$$

In general, the real part of ε^* vanishes near the plasma oscillation resonance frequency ω_{p}, so that with the use of Eq. (25), ω_{N}^2 can be given by

$$\omega_{\mathrm{N}}^2 = \varepsilon_\infty(\omega_{\mathrm{p}}^2 + \gamma^2) \tag{26}$$

Substituting Eq. (26) into Eq. (20), we have

$$\chi^{\mathrm{f}}(\omega) = -\varepsilon_\infty \frac{\omega_{\mathrm{p}}^2 + \gamma^2}{\omega^2 + \gamma^2} + i\varepsilon_\infty \frac{\omega_{\mathrm{p}}^2 + \gamma^2}{\omega}\,\frac{\gamma}{\omega^2 + \gamma^2} \tag{27}$$

In the low-frequency region ($\hbar\omega < 0.39$ eV), $\chi^{\mathrm{b}}(\omega)$ vanishes for metals. Using Eq. (27), the complex dielectric function from Eq. (19) becomes

$$\varepsilon^* = \varepsilon_1 + i\varepsilon_2 \approx 1 + \chi^{\mathrm{f}}(\omega) = 1 - \varepsilon_\infty \frac{\omega_{\mathrm{p}}^2 + \gamma^2}{\omega^2 + \gamma^2} + i\varepsilon_\infty \frac{\omega_{\mathrm{p}}^2 + \gamma^2}{\omega}\,\frac{\gamma}{\omega^2 + \gamma^2} \tag{28}$$

The plasma frequency of the metal, ω_{p}, in the above equations can be found in the literature.

Generally, at room temperature, quantum effects can be neglected, and so, taking into account the interaction of electrons, the damping frequency γ in the above equations can be written [14]

$$\gamma(T, \omega) = \gamma_0 \left[1 + \left(\frac{\hbar\omega}{2\pi k_{\mathrm{B}} T} \right)^2 \right] \tag{29}$$

where k_{B} is the Boltzmann constant, T is the absolute temperature, and γ_0 is the classical damping frequency and is frequency independent. A more detailed discussion and an expression for the damping frequency γ_0 were given with the form in Ref. 9, that is,

$$\gamma_0 = \sigma\,\frac{1 - \sqrt{1 - (2\omega_{\mathrm{p}}\varepsilon_0\varepsilon_\infty/\sigma)^2}}{2\varepsilon_0\varepsilon_\infty} \tag{30}$$

With a knowledge of γ and ω_p, $\varepsilon_1(\omega)$ and $\varepsilon_2(\omega)$ can be calculated, respectively, by

$$\varepsilon_1(\omega) = 1 - \varepsilon_\infty \frac{\omega_p^2 + \gamma^2}{\omega^2 + \gamma^2} \tag{31}$$

$$\varepsilon_2(\omega) = \varepsilon_\infty \frac{\omega_p^2 + \gamma^2}{\omega} \frac{\gamma}{\omega^2 + \gamma^2} \tag{32}$$

Then, with the optical constants, n and k, determined using Eqs. (16) and (17), the thermal radiative properties can be predicted based on the Fresnel equations.

3.2. The Complex Dielectric Function of Heavily Doped Oxide Semiconductors

The complex dielectric function of a heavily doped semiconductor was discussed in previous work [9] and can be expressed as follows:

$$\varepsilon_1 = \varepsilon_\infty - \frac{\omega_N^2}{\omega^2 + \gamma_0^2} = \varepsilon_\infty \left(1 - \frac{\omega_p^2 + \gamma_0^2}{\omega^2 + \gamma_0^2}\right) \tag{33}$$

$$\varepsilon_2 = \frac{\omega_N^2 \gamma_0}{\omega(\omega^2 + \gamma_0^2)} = \varepsilon_\infty \frac{\gamma_0}{\omega} \left(\frac{\omega_p^2 + \gamma_0^2}{\omega^2 + \gamma_0^2}\right) \tag{34}$$

$$\omega_p^2 = \frac{e^2 n_e}{\varepsilon_\infty \varepsilon_0 m_c^*} - \gamma_0^2 \tag{35}$$

where m_c^* is the effective mass of electrons.

The plasma frequency, ω_p, can be determined by the intersection of the transmittance and reflectance spectral curves in the range of $0.35 \leqslant \lambda \leqslant 2.5\,\mu$m [9], while the sheet resistance, $R_\square$, and the thickness, d, of the film can be measured experimentally. Then the electrical conductivity, σ, can be determined by $\sigma = 1/(R_\square d)$. The normal emissivity, ϵ_n, for ITO heat mirror films at $T = 333$ K was measured with a portable device developed by SIC, CAS [15].

4. RESULTS

The experimental results for the directional emissivity of aluminum at $T = 443$ K [8] reported by Schmidt and Eckert [4, 5, 8], the predicted results obtained using the D-R method, and the deviations ($\delta_{\text{D-R}}$) between them are presened in Table I. Results predicted by other methods and their

Table I. Comparison of the Experimental Directional Emissivity of Aluminum Obtained by Schmidt and Eckert [8] with Results Predicted by the D-R and Other Methods

Al	Angle (°)	Exp ($T = 423$ K)	D-R	$\delta_{\text{D-R}}$ (%)[a]	A[b]	δ_A (%)[a]	B[b]	δ_B (%)[a]	C[b]	δ_C (%)[a]	D[b]	δ_D (%)[a]
$\omega_p = 2.30 \times 10^{16}$ rad · s^{-1} [12]	0	0.039	0.042	7.69	0.022	−43.6	0.089	128.2	0.050	28.2	0.067	71.8
$\sigma = 2.11 \times 10^{7}\ \Omega^{-1} \cdot \text{m}^{-1}$ [16]	10	0.039	0.042	7.69	0.022	−43.6	0.089	128.2	0.050	28.2	0.067	71.8
$\varepsilon_\infty = 0.7$ [12]	20	0.039	0.042	7.69	0.022	−43.6	0.089	128.2	0.050	28.2	0.067	71.8
$\epsilon(\theta)$ calculated at $T = 423$ K	30	0.0395	0.042	6.32	0.022	−44.3	0.090	127.8	0.050	26.5	0.067	69.6
from 3.27 to 50.23 μm	40	0.04	0.043	7.50	0.022	−45.0	0.091	127.5	0.051	27.5	0.068	70
	50	0.0415	0.045	8.43	0.022	−46.9	0.095	128.9	0.053	27.7	0.071	71.1
	60	0.0496	0.048	−3.22	0.022	−55.6	0.103	107.7	0.057	14.9	0.076	53.2
	70	0.0605	0.055	−9.09	0.022	−63.6	0.124	104.9	0.067	10.7	0.090	48.8
	80	0.095	0.079	−16.8	0.022	−76.8	0.185	105.0	0.100	5.26	0.135	42.1
	82	—	0.090	—	0.023	—	0.210	—	0.115	—	0.156	—
	85	0.139	0.123	−11.5	0.024	−82.7	0.273	96.4	0.159	14.4	0.210	51.1
	85.8	—	0.139	—	0.025	—	0.296	—	0.179	—	0.240	—

[a] Deviations of prediction results from those of Schmidt and Eckert.
[b] Various prediction methods as described in Section 4.

deviations δ_x are also illustrated in the same table. These methods are as follows.

Method A: The results were obtained using the Hagen–Rubens relation and Fresnel equations [4, 5],

$$n = k \approx \sqrt{30\sigma\lambda_0} \tag{36}$$

$\epsilon(\theta)$ is then obtained using Eqs. (11)–(13) and (18).

Method B: Assuming $n = k$, Eqs. (11) and (12) become

$$R_{s\lambda}(\theta) = |\mathbf{r}_{s\lambda}|^2 = \frac{(n - \cos\theta)^2 + n^2}{(n + \cos\theta)^2 + n^2} \tag{37}$$

$$R_{p\lambda}(\theta) = |\mathbf{r}_{p\lambda}|^2 = \frac{(n\cos\theta - 1)^2 + (n\cos\theta)^2}{(n\cos\theta + 1)^2 + (n\cos\theta)^2} \tag{38}$$

Thus, $\epsilon_\lambda(\theta)$ can be calculated using Eqs. (13), (29)–(32), (37), and (38) combined with Eq. (18) to obtain $\epsilon(\theta)$.

Method C: Assuming $n = k$, and substituting k into Eqs. (11) and (12) as

$$R_{s\lambda}(\theta) = |\mathbf{r}_{s\lambda}|^2 = \frac{(k - \cos\theta)^2 + k^2}{(k + \cos\theta)^2 + k^2} \tag{39}$$

$$R_{p\lambda}(\theta) = |\mathbf{r}_{p\lambda}|^2 = \frac{(k\cos\theta - 1)^2 + (k\cos\theta)^2}{(k\cos\theta + 1)^2 + (k\cos\theta)^2} \tag{40}$$

Results were obtained using Eqs. (13), (18), (29)–(32), (39), and (40).

Method D: Assuming $n = k$, from Eq. (15)

$$n = k = \sqrt{0.5\varepsilon_2} \tag{41}$$

Results were obtained using Eqs. (11)–(13), (18), (29), (31), and (32).

Predicted results for Al and the experimental data reported by Schmidt and Eckert are plotted in Fig. 1 for comparison. Results of the directional emissivity of copper at $T = 293$ K are given in Table II. The methods used for obtaining the results in columns D-R, A, B, C, and D are the same as stated above.

Table III lists the predicted results of the total normal emissivity of aluminum at $T = 773$ K and copper at $T = 293$ K, the spectrum normal emissivity of copper at 4 μm and 293 K, and measured results from the literature.

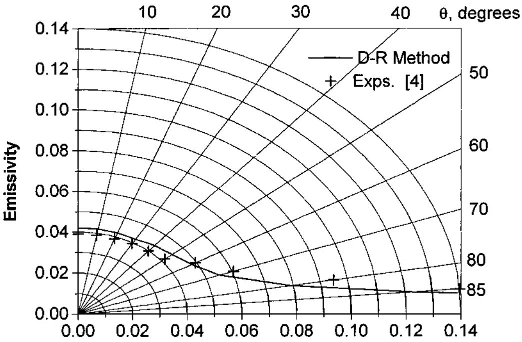

Fig. 1. Directional variation of surface emissivity for aluminum.

Table II. Directional Emissivity of Copper Predicted by the D-R and Other Methods

Cu	Angle (°)	D-R	A[a]	B[a]	C[a]	D[a]
$\omega_p = 1.13 \times 10^{16}$ rad $\cdot$ s^{-1} [11]	0	0.029	0.021	0.094	0.039	0.057
$\sigma = 5.81 \times 10^7$ $\Omega^{-1} \cdot$ m^{-1} [16]	10	0.029	0.021	0.094	0.039	0.057
$\varepsilon_\infty = 1.6$ [11]	20	0.029	0.021	0.094	0.039	0.057
$T = 293$ K	30	0.029	0.021	0.095	0.039	0.057
Calculated from 4.95 to	40	0.029	0.021	0.096	0.039	0.058
75.94 μm	50	0.030	0.021	0.100	0.040	0.060
	60	0.031	0.021	0.109	0.043	0.065
	70	0.034	0.022	0.130	0.049	0.077
	80	0.043	0.022	0.192	0.070	0.116
	85	0.063	0.022	0.278	0.109	0.182

[a] Various prediction methods as described in Section 4.

Table III. Results of Measurements and Predictions by the D-R Method for the Total Normal Emissivity of Al and Cu and the Spectrum Normal Emissivity of Cu at 4 μm

Sample	T (K)	$\epsilon_{n,\,\text{D-R}}$	$\epsilon_{n,\,\text{Exp}}$	$\epsilon_{n,\,\text{D-R},\,\lambda}$	$\epsilon_{n,\,\text{Exp},\,\lambda}$
Al	773	0.057	0.050[a]	—	—
Cu	293	0.029	0.030	—	—
Cu	293	—	—	0.0257	0.027[b]

[a] Data from Ref. 8.
[b] Data from Ref. 5 (p. 113).

Table IV. Data for ITO Films (Samples I, II, and III)[a]

Sample	ω_p (10^{15} rad · s^{-1})	$R\square$ ($\Omega/\square$)	d (10^{-6} m)	$\rho = \sigma^{-1}$ ($10^{-6}\,\Omega \cdot$ m)	ϵ_n (Exp)	ϵ_n (D-R)	A[b]	B[b]	C[b]	D[b]
I	1.02	9.0	0.48	4.32	0.190	0.193	0.049	0.363	0.226	0.289
II	1.18	5.2	0.57	2.96	0.160	0.163	0.041	0.336	0.190	0.269
III	1.36	3.7	0.78	2.89	0.158	0.166	0.040	0.299	0.192	0.240

[a] ω_p, plasma frequency; $R_\square$, sheet resistance; d, thickness; ρ and σ, resistivity and electrical conductivity, respectively; ϵ_n, normal emissivity.
[b] Various prediction methods as described in Section 4.

Table IV gives the room-temperature data on ω_p, $R_\square$, d, σ, and the emissivity of the samples, ϵ_n, for ITO heat mirror films deposited by RF sputtering onto 2-mm-thickness unheated glass. The methods used for obtaining the results in columns D-R, A, B, C, and D are the same as in Table I.

The deviation of the predicted result for Al from the experimental value is about 16.8% at $\theta = 80°$ and less than 11.5% at other angles. From the results predicted by the D-R method and the experimental results given by Schmidt and Eckert, we note that when θ is greater than 80° the variation of total directional emissivity with θ is quite sensitive. For this reason we think that an evident deviation in total directional emissivity can arise when there is little error in the determination of θ.

The values for the high-frequency dielectric constant ε_∞ of aluminum are reproduced in Table I. These values conflict with results given in Ref. 4 (Figs. 3–7, p. 93).

5. CONCLUSIONS

The success of the D-R method was verified by good agreement between predicted results for Al and experimental values given by Schmidt and Eckert, as shown in Table I and Fig. 1. It can also be seen in Table II that the results given by the D-R method are in agreement with those of experimental measurements, but the deviations of the results calculated by using the Hagen–Rubens relation or assuming $n = k$ from the experimental values are obvious. Hence, for predicting the thermal radiative properties of metals and heavily doped oxide semiconducting heat mirror films, the D-R method is recommended.

ACKNOWLEDGMENTS

The authors are grateful to Prof. Bu-Xuan Wang, Academician of the Chinese Academy of Science (Thermal Engineering Department, Tsinghua

University) for valuable comments and suggestions. Discussions with Dr. Zhuomin Zhang (Department of Mechanical Engineering, University of Florida) were very useful in understanding several aspects of this work.

REFERENCES

1. M. A. Bramson, *Infrared Radiation of Heated Bodies* ("Science" Publishing House, Moscow, 1964), pp. 97–99 (in Russian).
2. A. G. Blaoh, *Fundamentals of Radiative Heat Transfer* (State Power Engineering Publishing House, Moscow, 1962), pp. 57–61 (in Russian).
3. S. Frank, in *Elementary Theory of The Optical Properties of Solids*, *Solid State Physics*, *Vol. 15*, F. Seitz and D. Turnbull, eds. (Academic Press, London, 1963), pp. 348–349.
4. M. F. Modest, *Radiative Heat Transfer* (McGraw–Hill, New York, 1993), pp. 75–98.
5. R. Siegel and J. R. Howell, *Thermal Radiation Heat Transfer*, 2nd ed. (McGraw–Hill, New York, 1981), pp. 112–115.
6. H. L. Hartnagel, A. L. Dawer, A. K. Jain, and C. Jagadish, *Semiconducting Transparent Thin Films* (IPO, London, 1995), pp. 312–313.
7. G. Frank, E. Kauer, and H. Kostlin, *Thin Solid Films* **77**:108 (1981).
8. E. R. G. Eckert, in *Handbook of Heat Transfer—Fundamentals*, 2nd ed., W. M. Rohsenow, J. P. Hartnett, and E. N. Ganic, eds. (McGraw–Hill, New York, 1985).
9. J. Chen, X.-S. Ge, and X.-F. Hu, *Solar Energy Mater. Solar Cells* **55**:323 (1998).
10. O. S. Heavens, *Optical Properties of Thin Solid Films* (Butterworths, London, 1955), p. 53.
11. H. Ehrenreich and H. R. Philipp, *Phys. Rev.* **128**:1622 (1962).
12. H. Ehrenreich, H. R. Philipp, and B. Segall, *Phys. Rev.* **132**:1918 (1963).
13. I. Hamberg and C. G. Granqvist, *J. Appl. Phys.* **60**:123 (1986).
14. F. Abelès, *Optical Properties of Solids*, F. Abelès, ed. (North-Holland, Amsterdam, 1972), p. 109.
15. J. T. Xu, *Research Report* (Shanghai Institute of Ceramics, Chinese Academy of Science, 1992) (in Chinese).
16. N. B. Vargaftik, *Thermophysical Properties of Materials* (State Power Engineering Publishing House, Moscow, 1956), p. 277 (in Russian).